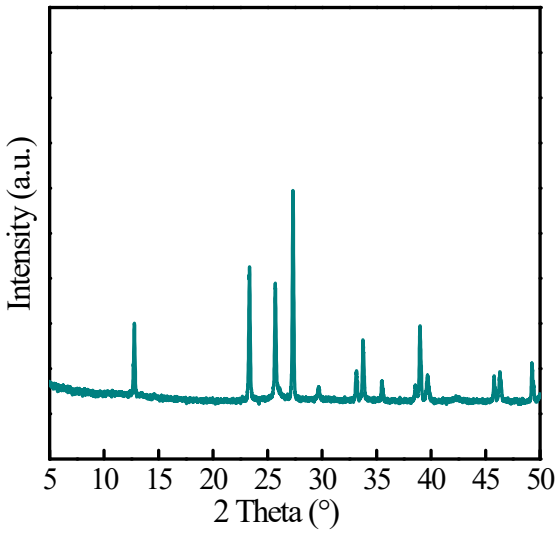

Fig. S1 XRD pattern of MoO_3 sample.

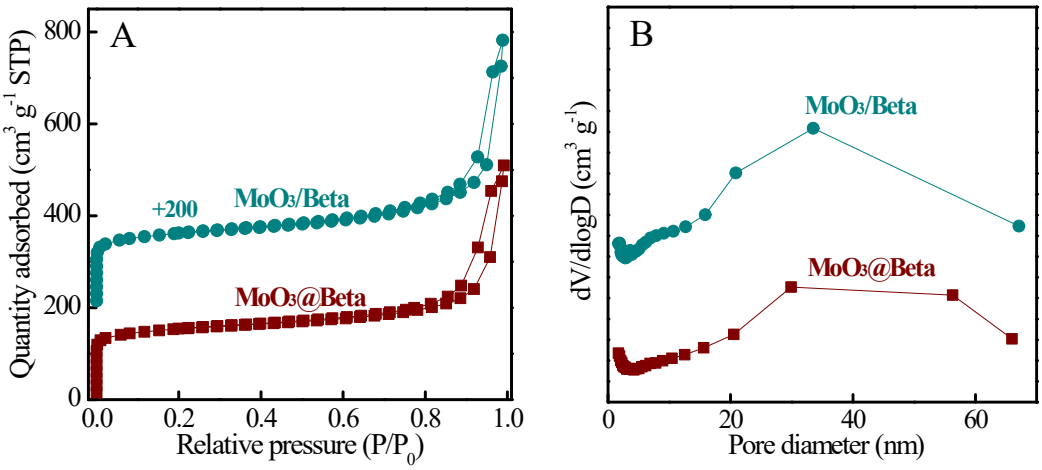

Fig. S2 (A) N_2 adsorption–desorption isotherms and (B) pore diameter distribution of MoO_3@Beta and MoO_3/Beta samples.

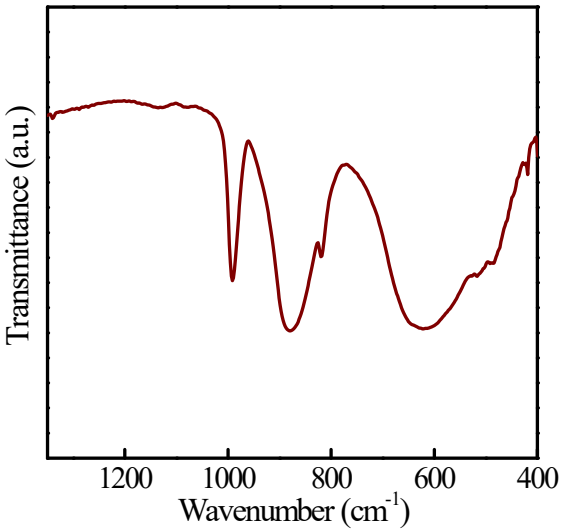

Fig. S3 FT-IR spectrum of MoO_3 sample.

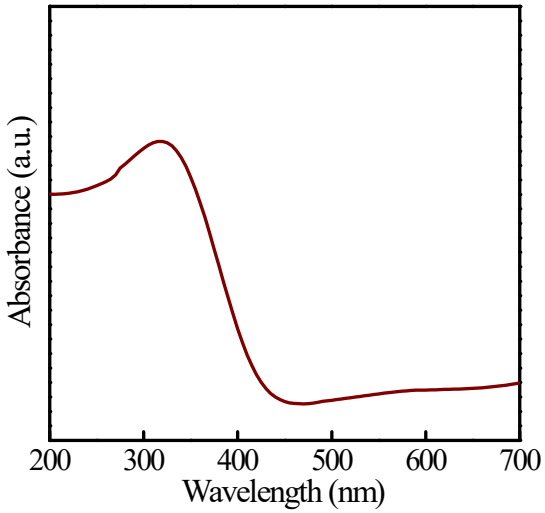

Fig. S4 UV-Vis spectrum of MoO_3 sample.

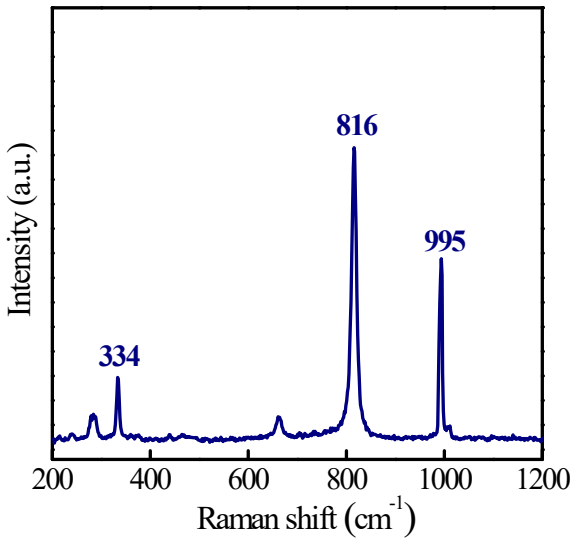

Fig. S5 UV Raman spectrum of MoO_3 sample.

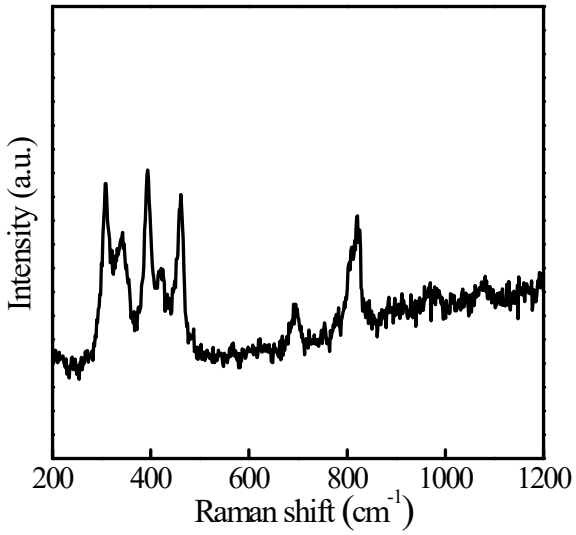

Fig. S6 UV Raman spectrum of Beta sample.

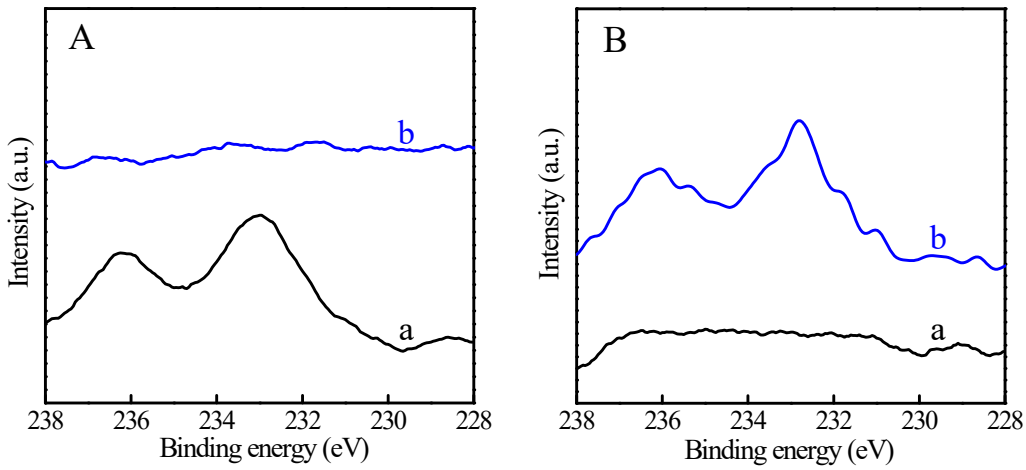

Fig. S7 Mo 3d XPS spectra with the etching depth of 0 nm (a) and 30 nm (b) over (A) MoO_3/Beta and (B) MoO_3@Beta samples.

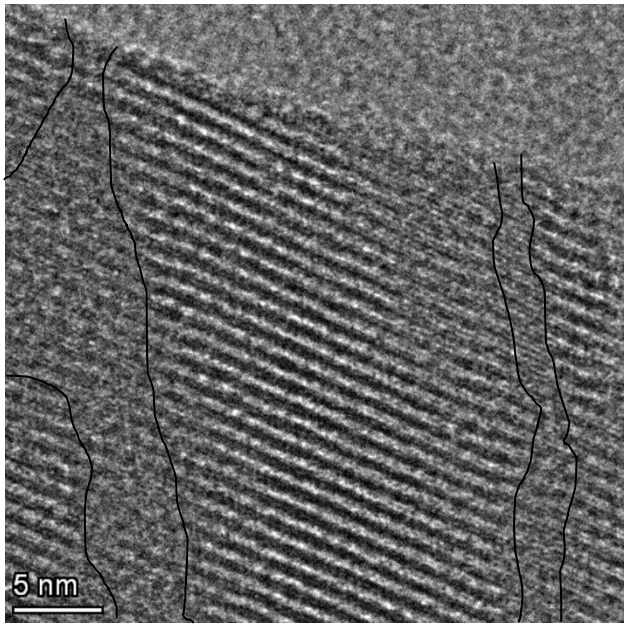

Fig. S8 High resolution TEM image of MoO_3@Beta sample. The yellow dash line indicated the presence of intracrystalline mesopores within zeolite crystal.

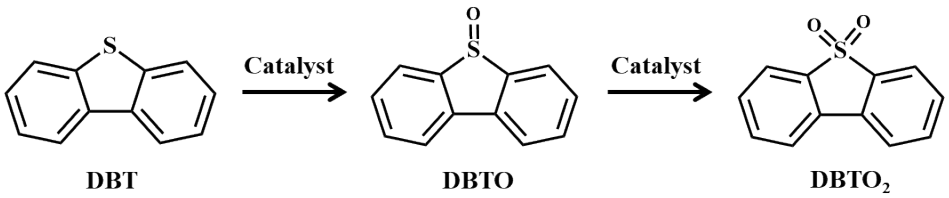

Scheme S1 Reaction pathways of DBT oxidation.

Table S1 Catalytic activity of various catalysts for oxidative desulfurization of DBT with molecular O_2.[a]

No.	Catalyst	Mo loading[b] (wt%)	Conversion[c] (%)
1	MoO_3	-	< 1.0
2	MoO_3/Beta	1.00	< 1.0
3	MoO_3@Beta	0.95	< 1.0

[a] Reaction conditions: catalyst, 0.02 g; model oil (S content, decalin, 500 μg mL^{-1}), 20 mL; O_2 pressure, 1 atm.; flow rate of O_2, 60 mL min^{-1}; temperature, 90 °C; time, 3 h.

[b] Calculated by ICP.

[c] Conversion = moles of DBT converted/initial moles of DBT × 100%.

Table S2 Comparison of TOF values over heterogeneous catalysts with the oxidant of O_2 or air.

Catalyst	Sulfide	Oxidant	Reaction conditions	Conversion (%)	TOF (h^{-1})	Ref.
Mo@Beta	DBT	O_2	90 °C, 1 mg/1 mL, 6 h	100	26.3	This work
Mo@Beta	DBT	O_2	100 °C, 1 mg/1 mL, 5 h	100	31.6	This work
CoMo nanosheet	DBT	air	80 °C, 10 mg/20 mL, 5 h	38.0	5.2	1
CoMo nanosheet	DBT	air	90 °C, 10 mg/20 mL, 5 h	70.0	9.6	1
CoMo nanosheet	DBT	air	100 °C, 10 mg/20 mL, 5 h	100.0	13.6	1
CoMo nanosheet	DBT	air	110 °C, 10 mg/20 mL, 2 h	100.0	34.1	1
Co-Mo-O	DBT	air	80 °C, 100 mg/20 mL, 9 h	75.0	0.2	2
Co-Mo-O	DBT	air	100 °C, 100 mg/20 mL, 6 h	82.0	0.4	2
Co-Mo-O	DBT	air	120 °C, 100 mg/20 mL, 3 h	100	0.9	2
Ce-Mo-O	DBT	air	80 °C, 100 mg/20 mL, 8 h	30.0	0.1	3
Ce-Mo-O	DBT	air	90 °C, 100 mg/20 mL, 8 h	50.0	0.1	3
Ce-Mo-O	DBT	air	100 °C, 100 mg/20 mL, 6 h	100	0.4	3
$Q_5IMo_6O_{24}$	DBT	O_2	80 °C, 10 mg/50 mL, 8 h	100	6.3	4
$Q_5IMo_6O_{24}$	DBT	O_2	85 °C, 10 mg/50 mL, 7 h	100	7.1	4
$Q_5IMo_6O_{24}$	DBT	O_2	90 °C, 10 mg/50 mL, 6 h	100	8.3	4
$Q_5IMo_6O_{24}$	DBT	O_2	100 °C, 10 mg/50 mL, 3 h	100	16.7	4
$Q_3Co(OH)_6Mo_6O_1$	DBT	O_2	80 °C, 11 mg/25 mL, 7 h	100	2.3	5
Pt/h-BN	DBT	air	110 °C, 50 mg/40 mL, 6 h	55.0	8.6	6
Pt/h-BN	DBT	air	120 °C, 50 mg/40 mL, 6 h	62.0	9.7	6
Pt/h-BN	DBT	air	130 °C, 50 mg/40 mL, 6 h	98.0	15.3	6
MoOx/MC-600	DBT	air	110 °C, 10 mg/20 mL, 8 h	43.3	0.7	7
MoOx/MC-600	DBT	air	115 °C, 10 mg/20 mL, 8 h	83.4	1.3	7
MoOx/MC-600	DBT	air	120 °C, 10mg/20 mL, 4 h	97.1	2.9	7
MIL-101(Cr)	DBT	O_2	120 °C, 5 mg/10 mL, 4 h	100	19.9	8
V_2O_5/BNNS	DBT	air	110 °C, 200 mg/50 mL, 4 h	72.4	0.6	9
V_2O_5/BNNS	DBT	air	120 °C, 200 mg/50 mL, 4 h	100	0.9	9
V_2O_5/BNNS	DBT	air	130 °C, 200 mg/50 mL, 3.5	100	1.0	9
V_8@iPAF	DBT	O_2	80 °C, 20 mg/6 mL, 5 h	100	1.0	10
3DOM WOx	DBT	air	120 °C, 10 mg/20 mL, 7 h	99.9	0.3	11
Atomic-layered	DBT	air	120 °C, 10 mg/50 mL, 10 h	99.7	1.8	12

(continued)

V_2O_5 BM-3	DBT	air	120 °C, 30 mg/50 mL, 4 h	99.7	0.6	13
$[C_8H_{17}N(CH_3)_3]_3$	DBT	O_2	90 °C, 40 mg/20 mL, 8 h	100	0.3	14
$[C_8H_{17}N(CH_3)_3]_3$	DBT	O_2	100 °C, 40 mg/20 mL, 1.25	100	1.7	14
$[C_8mim]_3H_3V_{10}O_2$	DBT	air	110 °C, 80 mg/40 mL, 4 h	67.4	1.6	15
$[C_8mim]_3H_3V_{10}O_2$	DBT	air	120 °C, 80 mg/40 mL, 4 h	99.8	2.4	15
$[C_8mim]_3H_3V_{10}O_2$	DBT	air	130 °C, 80 mg/40 mL, 4 h	100	2.4	15
$[C_8H_{17}N(CH_3)_3]_3$	DBT	O_2	100 °C, 40 mg/20 mL, 2.5 h	100	0.6	16
$Q_5H_4PV_{14}O_{42}$	DBT	O_2	90 °C, 40 mg/20 mL, 7 h	100	0.2	17
$Q_5H_4PV_{14}O_{42}$	DBT	O_2	100 °C, 40 mg/20 mL, 5 h	100	0.3	17
MFM-300(V)	DBT	O_2	120 °C, 3.75 mg/5 mL, 5 h	99.6	6.7	18

The column of 'Reaction conditions' contained reaction temperature (°C), catalyst dosage (mg), volume of model oil (mL), reaction time (h), respectively.

Turnover frequency (TOF, h^{-1}) was calculated as follows:

$$TOF(h^{-1}) = \frac{S_{conv} \times C_0 \times V_{oil}/t}{m \times \omega/M}$$

S_{conv}: conversion of sulfides;

C_0: initial sulfur content, mol L^{-1};

V_{oil}: volume of model oil, L;

t: reaction time, h;

m: mass of catalyst dosage, g;

ω: loading in the catalyst;

M: atomic mass of active metal, g mol^{-1}.

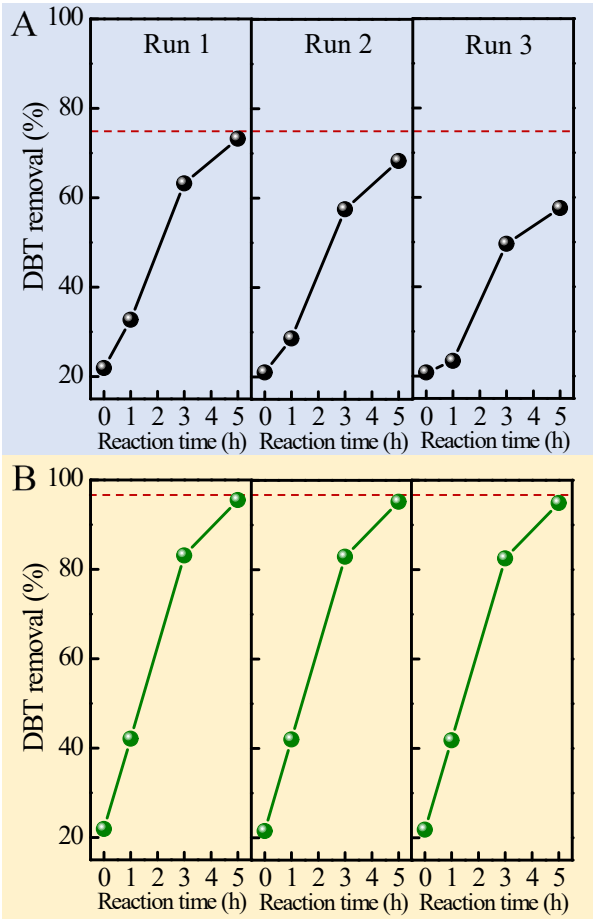

Fig. S9 Reusability of (A) MoO_3/Beta and (B) MoO_3@Beta catalysts in the DBT oxidation. The used catalysts were regenerated by calcination at 600 °C for 6 h after each run. Reaction conditions: model diesel (S content of 500 μg mL^{-1}), 20 mL; DES, 4 g; MoO_3@Beta, 0.02 g; temperature, 90 °C; O_2 pressure, 1 atm.; flow rate of O_2, 60 mL min^{-1}.

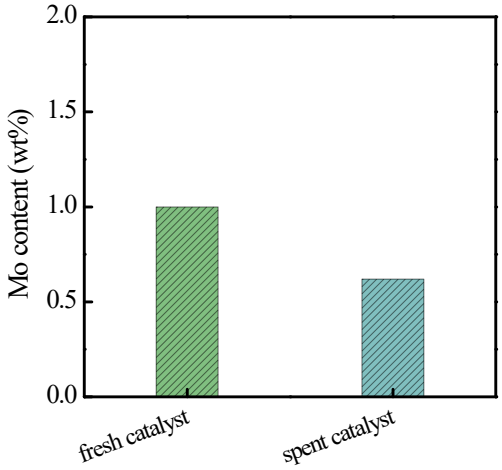

Fig. S10 Mo content for fresh and spent MoO_3/Beta catalyst.

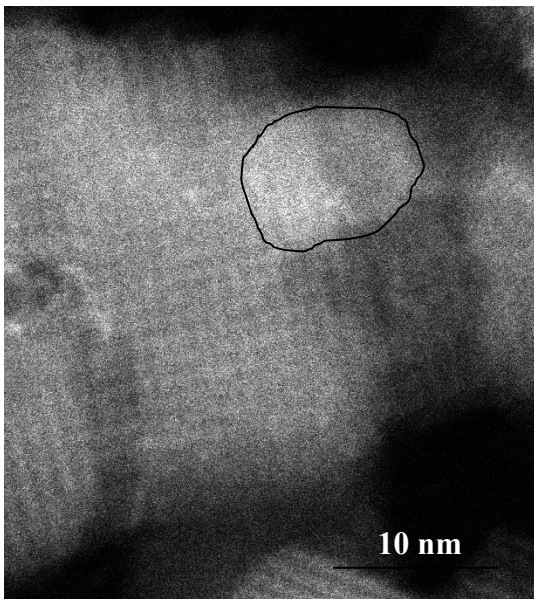

Fig. S11 AC-HAADF-STEM image of the spent MoO_3/Beta catalyst regenerated by calcination at 600 °C for 6 h.

Table S3 Catalytic activity of O_2-treated MoO_3@Beta for 3 h in oxidative desulfurization of DBT with molecular O_2.

No.	Catalyst	Mo loading[a] (wt%)	Conversion[b] (%)
1[c]	MoO_3@Beta[O]	0.95	< 1.0
2[d]	MoO_3@Beta[O]	0.95	< 1.0

[a] Calculated by ICP.

[b] Conversion = moles of DBT converted/initial moles of DBT × 100%.

[c] Reaction conditions: catalyst, 0.02 g; model oil (S content, decalin, 500 μg mL^{-1}), 20 mL; temperature, 90 °C; time, 5 h.

[d] Reaction conditions: catalyst, 0.02 g; model oil (S content, decalin, 500 μg mL^{-1}), 20 mL; O_2 pressure, 1 atm.; flow rate of O_2, 60 mL min^{-1}; temperature, 90 °C; time, 5 h.

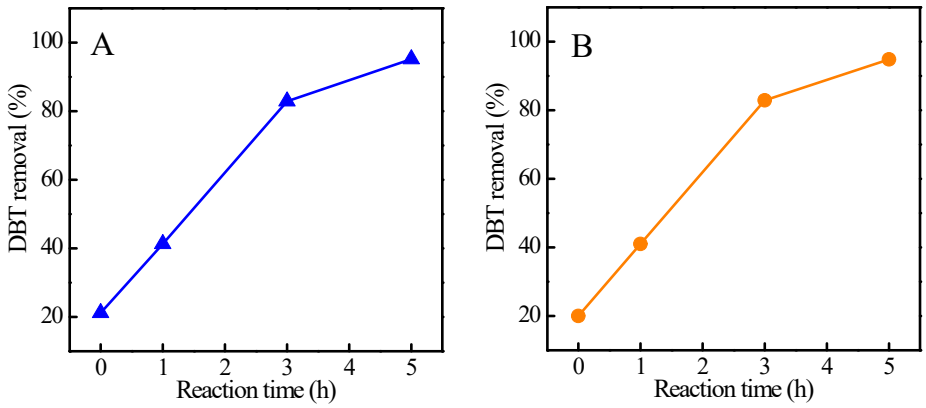

Fig. S12 Selective quenching experiments with (A) L-histidine and (B) ethanol. Reaction conditions: model diesel (S content of 500 μg mL^{-1}), 20 mL; DES, 4 g; MoO_3@Beta, 0.02 g; quencher, 50% mass ratio to DBT; temperature, 90 °C; O_2 pressure, 1 atm; flow rate of O_2, 60 mL min^{-1}.

References

[1] Y. Dong, J. Zhang, Z. Ma, H. Xu, H. Yang, L. Yang, L. Bai, D. Wei, W. Wang, H. Chen, Preparation of Co-Mo-O ultrathin nanosheets with outstanding catalytic performance in aerobic oxidative desulfurization, Chem. Commun. 55 (2019) 13995–13998, https://doi.org/10.1039/C9CC07452J.

[2] Q. Zhang, J. Zhang, H. Yang, Y. Dong, Y. Liu, L. Yang, D. Wei, W. Wang, L. Bai, H. Chen, Efficient aerobic oxidative desulfurization over Co–Mo–O bimetallic oxide catalysts. Catal, Sci. Technol. 9 (2019) 2915–2922, https://doi.org/10.1039/C9CY00459A.

[3] Y. Shi, G. Liu, B. Zhang, X. Zhang, Oxidation of refractory sulfur compounds with molecular oxygen over a Ce–Mo–O catalyst, Green Chem. 18 (2016) 5273–5279, https://doi.org/10.1039/C6GC01357K.

[4] H. Lv, Y. Zhang, Z. Jiang, C. Li, Aerobic oxidative desulfurization of benzothiophene, dibenzothiophene and 4,6-dimethyldibenzothiophene using an anderson-type catalyst $[(C_{18}H_{37})_2N(CH_3)_2]_5[IMo_6O_{24}]$, Green Chem. 12 (2010) 1954–1958, https://doi.org/10.1039/C0GC00271B.

[5] H. Lv, W. Ren, W. Liao, W. Chen, Y. Li, Z. Suo, Aerobic oxidative desulfurization of model diesel using a B-type anderson catalyst $[(C_{18}H_{37})_2N(CH_3)_2]_3Co(OH)_6Mo_6O_{18}\cdot 3H_2O$, Appl. Catal. B: Environ. (2013), 138–139, 79–83, https://doi.org/10.1016/j.apcatb.2013.02.034.

[6] P.W. Wu, Y.C. Wu, L.L. Chen, J. He, M.Q. Hua, F.X. Zhu, X.Z. Chu, J. Xiong, M.Q. He, W.S. Zhu, H.M. Li, Boosting aerobic oxidative desulfurization performance in fuel oil via strong metal-edge interactions between Pt and h-BN, Chem. Eng. J. 380 (2020) 122526, https://doi.org/10.1016/j.cej.2019.122526.

[7] W. Jiang, J. Xiao, L. Dong, C. Wang, H. Li, Y. Luo, W. Zhu, H. Li, Polyoxometalate-based poly (ionic liquid) as a precursor for superhydrophobic magnetic carbon composite catalysts toward aerobic oxidative desulfurization, ACS Sustain. Chem. Eng. 7 (2019) 15755–15761, https://doi.org/10.1021/acssuschemeng.9b04026.

[8] A. Gomez-Paricio, A. Santiago-Portillo, S. Navalon, P. Concepcion, M. Alvaro, H. Garcia, MIL-101 promotes the efficient aerobic oxidative desulfurization of dibenzothiophenes, Green Chem. 18 (2016) 508–515, https://doi.org/10.1039/C5GC00862J.

[9] C. Wang, Y. Qiu, H. Wu, W. Yang, Q. Zhu, Z. Chen, S. Xun, W. Zhu, H. Li, Construction of 2D-2D V_2O_5/BNNS nanocomposites for improved aerobic oxidative desulfurization performance, Fuel 270 (2020) 117498, https://doi.org/10.1016/j.fuel.2020.117498.

[10] J. Song, Y. Li, P. Cao, X. Jing, M. Faheem, Y. Matsuo, Y. Zhu, Y. Tian, X. Wang, G. Zhu, Synergic catalysts of polyoxometalate@cationic porous aromatic frameworks: reciprocal modulation of both capture and conversion materials, Adv. Mater. 31 (2019) 1902444, https://doi.org/10.1002/adma.201902444.

[11] M. Zhang, W. Liao, Y. Wei, C. Wang, Y. Fu, Y. Gao, L. Zhu, W. Zhu, H. Li, Aerobic oxidative desulfurization by nanoporous tungsten oxide with oxygen defects, Appl. Nano Mater. 4 (2021) 1085–1093, https://doi.org/10.1021/acsanm.0c02639.

[12] C. Wang, H.P. Li, X.J. Zhang, Y. Qiu, Q. Zhu, S.H. Xun, W.S. Yang, H.M. Li, Z.G. Chen, W.S. Zhu, Atomic-layered α-V_2O_5 nanosheets obtained via fast gas-driven exfoliation for superior aerobic oxidative desulfurization, Energy Fuels 34 (2020), 2612–2616, https://doi.org/10.1021/acs.energyfuels.9b04401.

[13] Y. Zou, C. Wang, H. Chen, H. Ji, Q. Zhu, W. Yang, L. Chen, Z. Chen, W. Zhu, Scalable and

facile synthesis of V_2O_5 nanoparticles via ball milling for improved aerobic oxidative desulfurization, Green Energy Environ. 6 (2021) 169–175, https://doi.org/10.1016/j.gee.2020.10.005.

[14] N.F. Tang, Y.N. Zhang, F. Lin, H.Y. Jiang, Z.X. Lu, C. Li, Oxidation of dibenzothiophene catalyzed by $[C_8H_{17}N(CH_3)_3]_3H_3V_{10}O_{28}$ using molecular oxygen as oxidant, Chem. Commun. 48 (2012) 11647–11649, https://doi.org/10.1039/C2CC36482D.

[15] C. Wang, Z.G. Chen, X.Y. Yao, Y.H. Chao, S.H. Xun, J. Xiong, L. Fan, W.S. Zhu, H.M. Li, Decavanadates anchored into micropores of graphene-like boron nitride: efficient heterogeneous catalysts for aerobic oxidative desulfurization, Fuel 230 (2018) 104–112, https://doi.org/10.1016/j.fuel.2018.04.153.

[16] N.F. Tang, Z.X. Jiang, C. Li, Oxidation of refractory sulfur-containing compounds with molecular oxygen catalyzed by vanadoperiodate, Green Chem. 17 (2015) 817–820, https://doi.org/10.1039/C4GC01790K.

[17] N.F. Tang, X.P. Zhao, Z.X. Jiang, C. Li, Oxidation of dibenzothiophene using oxygen and a vanadophosphate catalyst for ultra-deep desulfurization of diesels, Chinese J. Catal. 35 (2014) 1433–1437, https://doi.org/10.1016/S1872-2067(14)60194-7.

[18] X.L. Li, Y.L. Gu, H.Q. Chu, G. Ye, W. Zhou, W. Xu, Y. Y.Sun, MFM-300(V) as an active heterogeneous catalyst for deep desulfurization of fuel oil by aerobic oxidation, Appl. Catal. A: Gen. 584 (2019) 117152, https://doi.org/10.1016/j.apcata.2019.117152.